STIFFNESS MODELING OF TRIAXIALLY BRAIDED TEXTILE COMPOSITES

Joon-Hyung Byun

Composite Materials Lab, Korea Institute of Machinery and Materials
66 Sangnam-Dong, Changwon, Kyungnam, South Korea

SUMMARY: An analytic model based upon the unit cell was developed to predict geometric characteristics and three-dimensional engineering constants of 2-D (two-dimensional) triaxially braided textile composites. The crimp yarn angle and the fiber volume fraction were obtained from the geometric model. The elastic model utilizes the coordinate transformation and the averaging of stiffness and compliance constants based upon the volume of each reinforcement and matrix material. Seven different fabric architectures have been fabricated and tested in tensile load to verify the model. The classical lamination theory has also been applied to the braided composites to compare the predictions with the averaging method. Although two analytic approaches are well correlated with experimental results, the averaging method is more accurate when the braider yarn angle is small or when the bundle size of axial yarns is much larger than that of the braider yarns.

KEYWORDS: braided textile, unit cell, geometric model, stiffness model, engineering constants, coordinate transformation, fabric architecture, averaging method.

INTRODUCTION

The development of composite parts requires that the material selection and design process should be linked with manufacturing costs. The labor-intensive aspects of tape laying-up and slow production rate of autoclave process have limited the application of composite materials mostly to aerospace and military industry, where the performance was the most important factor. As the application areas of composite materials are steadily expanding, it is essential to develop the technology for designing and manufacturing the cost-effective structures. Even in the aerospace and military sectors, pressure on productivity and costs have been a major force. Recent advancements in liquid molding process, coupled with higher production rate of textile preforms have brought a renewed interest to textile structural composites. Among many types of textiles, braided preforms can provide a wide range of fiber orientations and preform cross-sections. Similar to the woven structure, the braided layer exhibits the yarn interlacing, which contributes structural stability during the braiding process and improves the damage tolerance of the composite parts. Due to the damage resistance and the manufacturing flexibility of near-net-shaping with high production rate, braided composites have been considered as a

candidate material for the aircraft structures [1]

In general, it is feasible to design textile composites with considerable flexibility in performance based upon wide variety of fiber architectures. Since there are many parameters involved in the mechanical properties of textile composites such as the fabric pattern, yarn bundle size, yarn types, and the yarn orientation angle, etc, it is necessary to develop a reliable model to analytically characterize the composites. Significant effort has been made in predicting the elastic properties of textile composites. But, compared with the achievements in modeling works on 2-D woven composites [2-6] very little work has been carried out on 2-D braided composites.

In this paper, the elastic model based upon the unit cell geometry and the averaging technique [7] has been established to predict the engineering constants of the triaxially braided composites. From the realistic description of the braid structure, the geometric parameters and the elastic constants are derived in closed-form expressions. The calculation procedures are simpler and easier to use than those based upon the lamination theory or the yarn discretization approach [8].

TRIAXIALLY BRAID STRUCTURE

A 2-D braided fabric consists of two sets of yarns passing over and under each other. In addition to the braiding yarns, axial yarns are often inserted for dimensional stability and improved mechanical properties in the longitudinal direction. Since the fiber directions are ±θ and 0 with respect to the longitudinal direction, this type of preform is called as a *triaxial* braid. Figure 1 (a) shows the schematic pattern of a regular braid to demonstrate the yarn interlacing. It can be seen that yarns pass over two and under two yarns oriented at opposite angles to each other. The pattern in Fig. 1 (a) seldom occurs in the actual braiding. Normally, the yarns are in contact with each other to make a compact structure as shown in Fig. 1 (b).

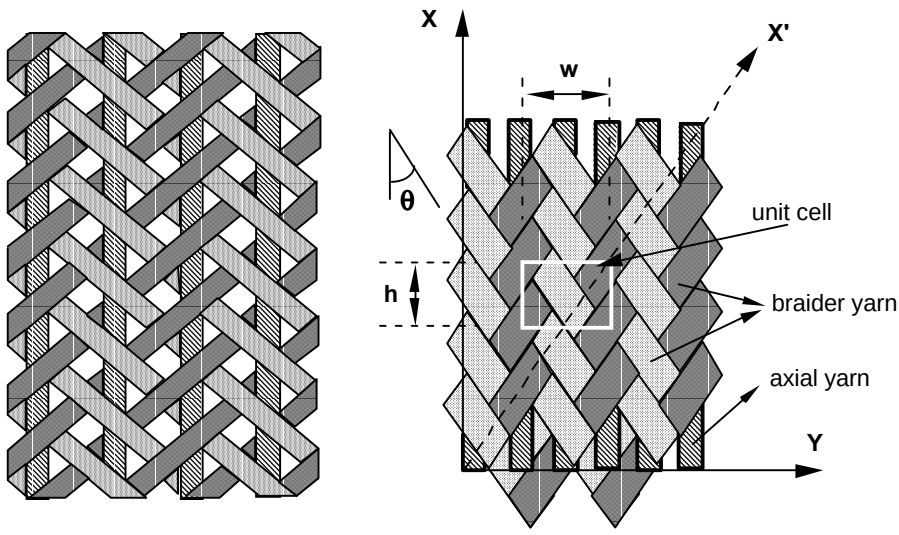

(a) (b)

Fig. 1: A triaxially braided preform; (a) schematic pattern;
(b) compact stucture.

The geometry of triaxial braids is characterized by the orientation of braider yarns, θ, and the pitch length, h. Due to the repeating motion of the carriers, braids have the smallest repeating structure termed as a *unit cell*. The line in Fig. 1 (b) indicates the unit cell, where two braider yarns at ±θ angles and two axial yarns are contained. The unit cell can be represented in the x-

y-z coordinate system. The x-axis is along the longitudinal direction or the length-wise axis. The braider yarn direction is denoted as x′-axis. The y-axis and z-axis are the width direction and thickness direction, respectively.

GEOMETRIC RELATION

Yarn Architecture

The yarn geometry is identified from the braid's microstructure. Figure 2 shows the yarn sections in the x′ direction. The letters 'A' and 'B' indicate the axial yarns and the braider yarns, respectively. The undulation section of braider yarns along the x′ direction shows a typical shape of yarn crimp. Due to the appearance of the yarn crimp and more regular shapes of yarn sections, the geometric model is based upon the section along the braider yarn direction. Figure 3 shows the schematic of the yarn sections and the yarn crimp. To describe the wavy geometry of the crossing yarn, the axial yarn cross section is assumed to be *lenticular* shape, which is the overlapped area of two circles. It is noted that the cross-section of braider yarns changes to irregular shape because they are located on the fabric surface, and tends to flatten when in contact with mold surfaces or other fabric layers.

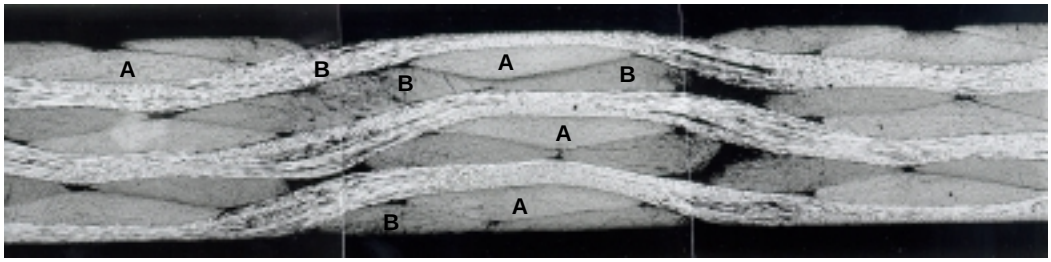

Fig. 2: Yarn sections in the braider yarn direction.

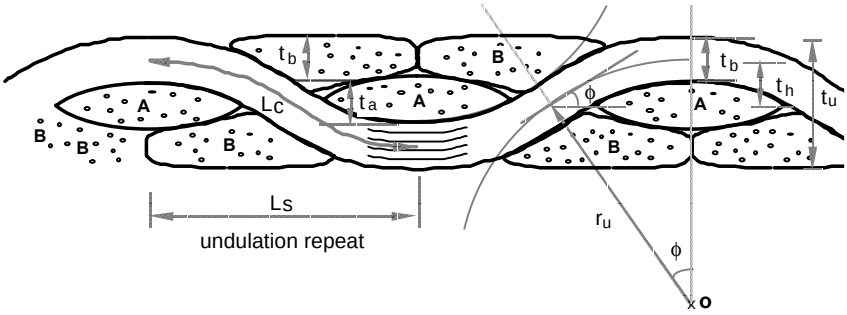

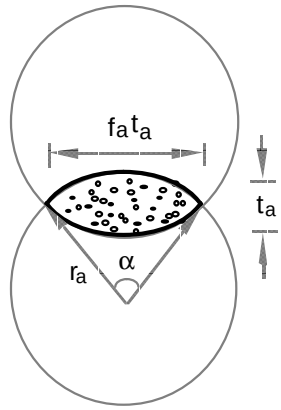

Fig. 3: Schematic of yarn sections in the braider yarn direction. Fig. 4: Cross-sectional shape.

Following parameters are defined to obtain the geometric relations: t_a , t_b , t_u = the thickness of axial yarns, braider yarns, and the unit cell, respectively; f_a = the aspect ratio of the axial yarn cross-section along the width directions (Fig. 4); L_s = the repeat length of the braider yarn undulation; r_u = the radius of the braider yarn undulation; and ϕ = the yarn crimp angle. Since the shape parameters of axial yarn, t_a and f_a can be measured from the sample photomicrograph, the following parameters can be determined from the known quantities.

$$L_s = \frac{h}{\cos\theta} \quad ; \quad t_b = \frac{t_u - t_a}{2} \quad ; \quad t_h = \frac{t_u - t_b}{2} \tag{1}$$

Since the shape of the axial yarn section is lenticular, the braider yarn undulation on it can be assumed to be an arc. It can be shown that the arc angle is the same as the yarn crimp angle. The radius of the braider yarn undulation and the crimp angle can be expressed as a function of parameters, L_s and t_h :

$$r_u = \frac{(L_s/2)^2 + t_h^2}{2t_h} \quad ; \quad \phi = \sin^{-1}\left(\frac{L_s}{2r_u}\right) \tag{2}$$

Since the yarn crimp angle has been determined, another important parameter for the geometric characteristics is the fiber volume fraction, which is treated in the following section.

Volume Calculation

Since the basic relations for the yarn architecture have been obtained, we are now ready to determine the fiber volume fraction of the braided composites. First, volumes of axial yarn and braider yarn in the unit cell are calculated by multiplying the area with the length of the yarn. Because the bundle sizes of axial and braider yarns are given when the preform is made, we can confine the calculation of the yarn area to the axial yarns only. The area of the braider yarn is expressed as a fraction or a multiple of axial yarn area.

Because of the regular shape of axial yarn cross-section the area is calculated in the width direction of the sample. Denoting α as the inner angle of the lenticular shape (Fig. 4), the cross-sectional area of the yarn can be expressed as :

$$A_a = r_a^2(\alpha_a - \sin\alpha_a) \; ; \; r_a = \frac{t_a}{4}(1 + f_a^2) \; ; \; \alpha_a = 2\sin^{-1}\left(\frac{2f_a}{1+f_a^2}\right) \tag{3}$$

Thus, volumes of axial yarns (V_a) and braider yarns (V_b) are determined from the yarn cross-sectional area, the yarn length, and the number of axial and braider yarns within the unit cell:

$$V_a = 2hA_a \; ; \; V_b = 4A_a\lambda L_c \tag{4}$$

where λ is the bundle size ratio of braider yarn to the axial yarn, and the undulation length of the braider yarn, L_c, is $2r_u\phi$. Denoting w as the width of the unit cell (Fig. 1 (b)), the fiber volume fraction is expressed as:

$$V_f = V_y\kappa = \frac{V_a + V_b}{hwt_u} \tag{5}$$

It should be noted that the yarn volume fraction is multiplied by a fiber packing fraction, κ, which is the local fiber volume fraction of a yarn bundle. The fiber packing fractions for the axial and braider yarns are assumed same.

Since the axial yarn content is directly connected with the mechanical property of the composites in the longitudinal direction, determination of this is important in designing the braided preform. The percentage of the axial yarn content (v_a) with respect to the total volume of the braid can be approximated as

$$v_a = \frac{V_a}{V_a + V_b} = \frac{\cos\theta}{\cos\theta + 2} \tag{6}$$

ELASTIC CONSTANTS

Coordinate Transformation

Figure 6 shows the coordinate systems of a crimp yarn. The local coordinate system is indicated as 1-2-3, where axis 1 coincides with fiber direction. In the global coordinate system, x′-axis is in the braider yarn direction, and z-axis is in the thickness direction of the composites. The basic assumption in the analysis is that the yarns are considered unidirectional composite rods after resin impregnation. The compliance matrix of the composite rod in the 1-2-3 coordinate system is expressed as follows due to the transverse isotropy:

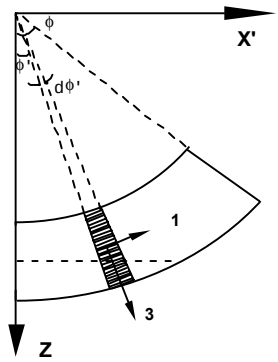

Fig. 5: Coordinate systems of a crimp yarn.

$$[S] = \begin{bmatrix} 1/E_{11} & -\nu_{21}/E_{22} & -\nu_{21}/E_{22} & 0 & 0 & 0 \\ -\nu_{12}/E_{11} & 1/E_{22} & -\nu_{32}/E_{22} & 0 & 0 & 0 \\ -\nu_{12}/E_{11} & -\nu_{23}/E_{22} & 1/E_{22} & 0 & 0 & 0 \\ 0 & 0 & 0 & 1/G_{23} & 0 & 0 \\ 0 & 0 & 0 & 0 & 1/G_{12} & 0 \\ 0 & 0 & 0 & 0 & 0 & 1/G_{12} \end{bmatrix} \tag{7}$$

The Young's and shear moduli are obtained from the fiber and matrix properties using micro-mechanics analysis [9]. Since the braider yarns have a crimp in the thickness direction, its deformation properties in the 1-2-3 coordinate system are transformed to the x′-y-z reference coordinate system. From the direction cosines between the x-y-z coordinate system and the 1-2-3 coordinate system, following transformation matrix can be established:

$$[T^c] = \begin{pmatrix} m^2 & 0 & n^2 & 0 & -2mn & 0 \\ 0 & 1 & 0 & 0 & 0 & 0 \\ n^2 & 0 & m^2 & 0 & 2mn & 0 \\ 0 & 0 & 0 & m & 0 & n \\ mn & 0 & -mn & 0 & m^2 - n^2 & 0 \\ 0 & 0 & 0 & -n & 0 & m \end{pmatrix}$$

(8)

where m = cosϕ and n = sinϕ. Thus, the compliance matrix of the unidirectional composite rod, referring to the 1-2-3 coordinate system, is transformed to [S'], referring to the x-y-z coordinate system:

$$[S'] = [T^c]^t\,[S][T^c] \tag{9}$$

where $[T^c]^t$ is a transpose matrix of $[T^c]$. The effective compliance matrix of a crimp yarn can be obtained by averaging the transformed compliance matrix of the infinitesimal yarn segment through the crimp angle, ϕ.

$$S_{ij}^c = \frac{1}{\phi}\int_0^{\phi'} S_{ij}^{'}\, d\phi' \qquad (i, j = 1-6) \tag{10}$$

Carrying out the integration gives the following results:

$$\begin{aligned}
&S_{11}^c = U_1 + (U_2/2\phi)\sin 2\phi + (U_3/4\phi)\sin 4\phi \\
&S_{12}^c = U_6 + (U_7/2\phi)\sin 2\phi \;\; ; \; S_{13}^c = U_4 - (U_3/4\phi)\sin 4\phi \\
&S_{15}^c = -(U_2 \sin^2\phi + U_3 \sin^2 2\phi)/\phi \;\; ; \; S_{22}^c = S_{22} \\
&S_{23}^c = U_6 - (U_7/2\phi)\sin 2\phi \;\; ; \; S_{25}^c = -(2U_7/\phi)\sin^2\phi \\
&S_{33}^c = U_1 - (U_2/2\phi)\sin 2\phi + (U_3/4\phi)\sin 4\phi \\
&S_{35}^c = -(U_2 \sin^2\phi - U_3 \sin^2 2\phi)/\phi \\
&S_{44}^c = U_8 + (U_9/2\phi)\sin 2\phi \;\; ; \; S_{46}^c = (U_9/2\phi)\sin^2\phi \\
&S_{55}^c = 4U_5 - (U_3/\phi)\sin 4\phi \;\; ; \; S_{66}^c = U_8 - (U_9/2\phi)\sin 2\phi \\
&S_{14}^b = S_{16}^b = S_{24}^b = S_{26}^b = S_{34}^b = S_{36}^b = S_{45}^b = S_{56}^b = 0
\end{aligned} \tag{11}$$

where

$$\begin{aligned}
&U_1 = (3S_{11} + 3S_{33} + 2S_{13} + S_{55})/8 \;\; ; \; U_2 = (S_{11} - S_{33})/2 \\
&U_3 = (S_{11} + S_{33} - 2S_{13} - S_{55})/8 \;\; ; \; U_4 = (S_{11} + S_{33} + 6S_{13} - S_{55})/8 \\
&U_5 = (S_{11} + S_{33} - 2S_{13} + S_{55})/8 \;\; ; \; U_6 = (S_{12} + S_{32})/2 \\
&U_7 = (S_{12} - S_{32})/2 \;\; ; \; U_8 = (S_{44} + S_{66})/2 \;\; ; \; U_9 = (S_{44} - S_{66})/2
\end{aligned} \tag{12}$$

The components in Eqn. (11) are the compliances of braider yarn composites in x′-y-z coordinate system. In order to transform these quantities into the x-y-z coordinate system of our interest, the same transformation rule in Eqn. (9) is applied.($p = \cos\theta$, $q = \sin\theta$)

$$[S^b] = [T^b]^t\,[S^c][T^b] \qquad \text{where } [T^b] = \begin{pmatrix} p^2 & q^2 & 0 & 0 & 0 & 2pq \\ q^2 & p^2 & 0 & 0 & 0 & -2pq \\ 0 & 0 & 1 & 0 & 0 & 0 \\ 0 & 0 & 0 & p & -q & 0 \\ 0 & 0 & 0 & q & p & 0 \\ -pq & pq & 0 & 0 & 0 & p^2 - q^2 \end{pmatrix} \tag{13}$$

Volume Averaging

Since the triaxially braided textile composites consist of four elements: braider yarns of $\pm\theta$ orientations, axial yarns, and matrix materials, it can be considered as a four-layered structure of different materials. In the unit cell, these layers are arranged in parallel in the longitudinal direction. When load is applied in the x-direction of the composites, each layer can be assumed to be in the state of constant strain. Thus, the stiffness of each layer is averaged based upon the volume to get the effective stiffness of the composites.

Because axial yarns are straight, the effective compliance is the same as Eqn. (7). For the determination of the effective stiffness of the composites, the compliance of axial and braider yarns are inverted to stiffness, and then are averaged over the unit cell volume.

$$C_{ij} = C_{ij}^{a}\frac{V_a}{V_t} + C_{ij}^{bp}\frac{V_b}{2V_t} + C_{ij}^{bm}\frac{V_b}{2V_t} + C^{m}(1-V_y) \qquad (i, j = 1-6) \tag{14}$$

where V_y is defined in Eqn. (5). C^{a}_{ij}, C^{bp}_{ij}, and C^{bm}_{ij} are the inverted stiffness of axial and braider yarns of $\pm\theta$ orientations, respectively. C^{m} is the [6x6] stiffness matrix of the matrix material. Then, the stiffness in Eqn. (14) is inverted to the compliance, S_{ij}, which finally results in the following engineering constants of the triaxially braided textile composites:

$$\begin{aligned} &E_{xx} = 1/S_{11}^{c}\ ;\ E_{yy} = 1/S_{22}^{c}\ ;\ E_{zz} = 1/S_{33}^{c};\\ &G_{yz} = 1/S_{44}^{c}\ ;\ G_{xz} = 1/S_{55}^{c}\ ;\ G_{xy} = 1/S_{66}^{c};\\ &\nu_{xy} = -S_{12}^{c}/S_{11}^{c}\ ;\ \nu_{zx} = -S_{13}^{c}/S_{33}^{c}\ ;\ \nu_{yz} = -S_{23}^{c}/S_{22}^{c} \end{aligned} \tag{15}$$

MODEL VERIFICATION

Sample Preparation

The triaxial braids were fabricated using T700S carbon fibers. By varying the fiber bundle size and the braid angle, seven different architectures were fabricated. Because only 12K bundle is available for T700S fiber, the size was varied as 12K, 24K, and 36K by putting two or three bundles together. For a fixed bundle size of 12K, three braider yarn angles was selected: 30°, 45°, and 60°. Table 1 specifies the identification code of the selected architectures in this study. The first character designates the bundle size of the axial yarn, and the second one for the braider yarns. The bundle sizes are designated as S(small), M(medium), and L(large) for the 12K, 24K, and 36K, respectively. The braided preforms were consolidated with epoxy resin by the resin transfer molding process. The samples were cured at 120°C for two hours.

Experiment and Input Data

The geometric model was verified with respect to the crimp angle and the fiber volume fraction. They were measured from photomicrographs and by the acid digestion method, respectively. The yarn packing fraction has been obtained by iteration calculation until the fiber volume fractions of the prediction and the experiment coincide with each other.

In order to verify the elastic model, tensile tests have been conducted for the straight-sided coupons with tabs. Specimens were instrumented with biaxial gages. The gage length was 10mm, and the width was 3mm. Although the gage didn't cover the whole unit cell, it was much longer than the length of the unit cell as indicated in Table 1. This satisfies the gage selection criterion [10] for this material, which requires that the gage length should at least equal the length of the unit cell in the loading direction.

The geometric input data for the model predictions were obtained from the photomicrographs of the sample section. Table 2 summarizes the input data of sample geometry and the mechanical properties of fibers and matrix.

Table 1: Yarn architectures of braids

Architecture Code	Axial Bundle Size (K)	Braider Bundle Size (K)	Braider Angle (deg.)	No. of Layers	Axial Yarn Vol. Content	Unit Cell Size, hwt_l (mm)
SS30	12	12	30	3	0.3	4.67 / 5.73 / 0.85
SS45	12	12	45	3	0.26	3.81 / 7.30 / 0.84
SS60	12	12	60	3	0.2	3.0 / 10.5 / 0.82
SM45	12	24	45	2	0.15	4.82 / 8.71 / 1.13
SL45	12	36	45	2	0.1	5.39 / 10.43 / 1.3
MS45	24	12	45	2	0.4	4.24 / 8.50 / 1.14
LS45	36	12	45	2	0.5	4.51 / 8.54 / 1.29

Table 2: Input data for the model prediction

Architecture Code	Geometric Data			Mechanical Data	
	t_a (mm)	f_a	λ	Carbon Fiber	Epoxy
SS30	0.49	3.14	1	E_{1f} = 230 (GPa)	E_m = 4 (GPa)
SS45	0.39	4.72	1	E_{2f} = 40.0 (GPa)	ν_m = 0.35
SS60	0.38	5.28	1	G_{12f} = 24 (GPa)	
SM45	0.49	3.72	2	G_{23f} = 14.3 (GPa)	
SL45	0.46	4.48	3	ν_{12f} = 0.26	
MS45	0.67	3.69	0.5		
LS45	0.95	2.60	0.33		

Table 3: Comparison of geometric parameters

Architecture Code	Crimp Angle ϕ (deg.)		Fiber Vol. Content V_f (%)		Fiber Packing Fraction, κ
	Measured	Predicted	Measured	Predicted	
SS30	16.5	14.2	53.9	53.6	0.77
SS45	14.2	13.0	45.1	44.9	0.74
SS60	14.3	11.4	46.4	46.3	0.77
SM45	16.2	13.6	61.7	61.8	0.75
SL45	17.6	13.1	61.8	61.6	0.70
MS45	16.2	17.2	40.3	40.5	0.72
LS45	35.0	20.0	42.8	42.4	0.74

Correlation

Table 3 summarizes the comparison between the model predictions and the test results for the geometric parameters. For the validation of these data, image analysis has been conducted for selected samples, which resulted in the range between 0.7 and 0.8.

The predicted angle of the yarn crimp was consistently smaller than the measured data. This may be due to the fact that the geometric model assumes one layer of the braid, and the yarn undulation of the multiple layers stacking is in-phase. In this case, the yarns tend to compress each other in the thickness direction, resulting in the lower angle of the braider yarn. Figure 2 shows the in-phase stacking of layers for the architecture type, SS45, and the measured and the predicted data were better correlated than the types, SS30 and SS60.

The architecture of triaxial braid is similar to the [0/±θ] laminates as far as the in-plane direction of the reinforcement is concerned. As a simple approximation method to predict the elastic properties, the classical lamination theory has been applied to the braid composites. Layup of laminates is the same as [0/±θ] with different lamina thickness. The thickness of 0

and ±θ laminae was calculated as the volume percentage of axial and braider yarns, respectively (Table 1). The fiber volume fraction of each type of laminate was set as the overall fiber volume fraction of the braided composites.

The data summarized in Tables 1 and 2 and the fiber packing fraction in Table 3 have been utilized to predict the elastic constants of the braided composites. Figure 7 and 8 show the comparison between and experimental results of tensile tests and the model predictions based upon the averaging method and the lamination theory. Relatively good agreement between the model predictions and the test results can be observed. It is surprising that the lamination theory is correlated well although it doesn't take into account the yarn undulation. This is due to the fact that the yarn undulation in the thickness direction has little effect on the in-plane properties of the composites when the braider yarn angle is relatively small. It can be seen that the lamination theory in the case of LS45 architecture, where the braider angle is quite large, over-predicts the Young's modulus. The yarn undulation, however, increases the through-the-thickness property, which directly reflects the improvement of impact property of the braided composites. Although the experimental data was not enough to support the predictions due to the limited test results, the methodology proposed in this paper can be effectively utilized in obtaining the three-dimensional elastic constants of the braided textile composites.

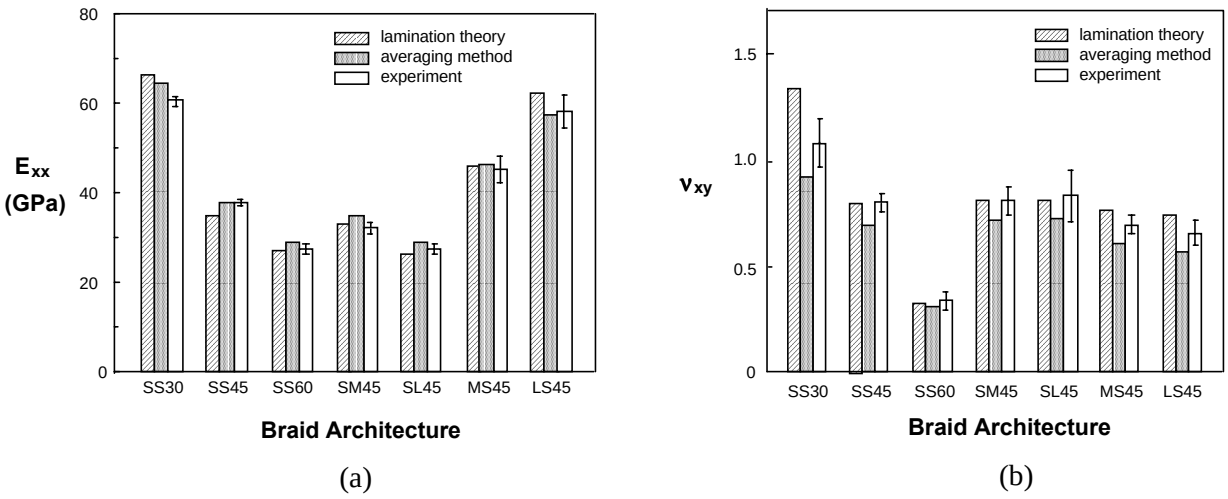

Fig. 6: Comparison between the model predictiona and the test results:
(a) Young's moduli and (b) Poisson's ratios.

CONCLUSION

(1) The geometric characteristics and the engineering constants of 2-D braided textile composites have been predicted based upon the analytic model. The crimp yarn angle, the axial yarn content, and the fiber volume fraction were obtained from the geometric model. Using the geometric parameters, three-dimensional engineering constants have been determined from the elastic model, which utilizes the coordinate transformation and the averaging of stiffness and compliance constants based upon the volume of each reinforcement and matrix material.

(2) In order to verify the model, seven different fabric architectures have been fabricated and tested in tensile mode. The longitudinal Young's modulus and the Poison's ratio have been obtained. The classical lamination theory has also been applied to compare the predictions with the averaging method. Relatively good agreement has been observed between the model predictions and the test results of carbon/epoxy composite samples.

Although these two analytic approaches are well correlated with experimental results, the averaging method is more accurate when the braider yarn angle is small or when the bundle size of axial yarns is much large than that of the axial yarns.

REFERENCES

1 Deaton, J. W., Dexter, H. B., Markus, A., and Rohwer K., Evaluation of braided stiffener concepts for transport aircraft wing structure applications. *NASA Conference Publication 3311 Part 1*, 1995, pp. 61–97.

2 Ishikawa, T. and Chou, T.-W., Stiffness and strength behavior of woven fabric composites. *J. Mater. Sci*., Vol. 17, 1982, pp. 3211-3220.

3 Ishikawa, T. and Chou, T.-W., Elastic behavior of woven hybrid composites. *J. Compos. Mater*.,Vol. 16, 1982, pp. 2-19.

4 Naik, N. K. and Shembekar, P. S., Elastic behavior of woven fabric composites: I-Lamina analysis, *J. Compos. Mater*., Vol. 16, 1992, pp. 2197-2225.

5 Woo, K. and Whitcomb, J. D., Three-dimensional failure analysis of plain weave textile composites using a global/local finite element method, *J. Compos. Mater*., Vol. 30, 1996, pp. 984-1003.

6 Dasgupta, A., Agarwal, R. K., and Bhandarkar, S. M., Three-dimensional modeling of woven fabric composites for effective thermo-mechanical and thermal properties, *Comp. Sci. Technol*., Vol. 56, 1996, pp. 209-223.

7 Kregers, A. F. and Teters, G. A., Use of averaging methods to determine the viscoelastic properties of spatially reinforced composites, *Mech. Compos. Mater*., Vol. 4, 1979, pp. 617–624.

8 Naik, R. A., Ifju, P. G., and Masters, J. E., Effect of fiber architecture parameters on deformation fields and elastic moduli of 2-D braided composites. *J. Compos. Mater*., Vol. 28, 1994, pp. 656–681.

9 Chou, T-W. *Microstructural design of fibrous composites*, Cambridge University Press, Cambridge, 1992.

10 Masters, J. E. and Ifju, P. G, Strain gage selection criteria for textile composite materials, *J. Compos. Technol. Res*., Vol. 19, 1997, pp. 152-167.